CHLORITE, CORRENSITE, AND CHLORITE-MICA IN LATE JURASSIC FLUVIO-LACUSTRINE SEDIMENTS OF THE CAMEROS BASIN OF NORTHEASTERN SPAIN

JOSÉ F. BARRENECHEA,[1] MAGDALENA RODAS,[1] MARTIN FREY,[2] JACINTO ALONSO-AZCÁRATE,[3] AND JOSÉ RAMÓN MAS[4]

[1] Departamento de Cristalografía y Mineralogía, Universidad Complutense de Madrid, 28040 Madrid, Spain
[2] Mineralogisch-Petrographisches Institut, Basel University, CH 4056 Basel, Switzerland
[3] Facultad Ciencias del Medio Ambiente, Universidad de Castilla-La Mancha, Fábrica de Armas, 45071 Toledo, Spain
[4] Departamento de Estratigrafía, Universidad Complutense de Madrid, 28040 Madrid, Spain

Abstract—The distribution and crystal-chemical characteristics of chlorite, corrensite, and mica in samples from a stratigraphic profile in the Cameros basin are controlled by changes in the sedimentary facies. The lacustrine marls and limestones from the base and the top of the profile contain quartz + calcite + illite ± dolomite ± chlorite ± albite ± paragonite ± Na, K-rich mica. Chlorite is rich in Mg, with Fe/(Fe + Mg) ratios ranging between 0.18–0.37. A formation mechanism involving reaction between Mg-rich carbonate and dioctahedral phyllosilicates is proposed for these Mg-rich chlorites, on the basis of the mutually exclusive relationship found between Mg-rich chlorite and dolomite, together with the relative increase in the proportion of calcite in samples containing chlorite.

The mudrocks from the middle part of the profile are composed of quartz + albite + illite + corrensite (with a mean coefficient of variability of 0.60%) ± chlorite. Corrensite and chlorite are richer in Fe^{2+} than those from the base or top of the profile, with mean Fe/(Fe + Mg) ratios of 0.51 and 0.56, respectively. Textural and compositional features suggest a formation mechanism for the corrensite, chlorite, and chlorite-mica crystals through replacement of detrital igneous biotite. Whether or not corrensite occurs with chlorite appears to be related to redox conditions. The presence of corrensite alone is apparently favored by oxidizing conditions, whereas the occurrence of corrensite + chlorite is related to more reducing conditions. Corrensite shows higher Si and Na + K + Ca contents, and slightly lower Fe/(Fe + Mg) ratios than chlorite. The presence of corrensite and the lack of random chlorite-smectite interlayering is discussed in terms of the fluid/rock ratio; the occurrence is related to the hydrothermal character of metamorphism in the Cameros basin.

Key Words—Cameros Basin, Chlorite, Chlorite-Mica, Corrensite, EMPA, Low-Grade Metamorphism, Sedimentary Facies, Spain, XRD.

INTRODUCTION

Chlorite and corrensite (1:1 regular interstratification of chlorite and smectite) occurrences have been described in different geological contexts. Both phases are commonly found as a product of hydrothermal alteration of various types of igneous rocks (Meunier *et al.,* 1988; Shau *et al.,* 1990; Shau and Peacor, 1992; Schiffman and Staudigel, 1995; Bettison-Varga and Mackinon, 1997; Schmidt and Robinson, 1997) or related to diagenesis of volcanoclastic sedimentary materials (Almon *et al.,* 1976; Chang *et al.,* 1986; Jiang and Peacor, 1994a, 1994b). In addition, they are frequently associated with ancient marine evaporites (Bodine and Madsen, 1987) or lacustrine mudrocks (April, 1981; Hillier, 1993).

In most occurrences, a sequence of transformation from smectite to corrensite and chlorite is observed, either by hydrothermal alteration in active geothermal fields (Schiffman and Staudigel, 1995) or by diagenetic reactions (Chang *et al.,* 1986; April, 1981). However, corrensite and chlorite may also form by replacement of biotite (Jiang and Peacor, 1994a, 1994b; Li *et al.,* 1998) and amphibole (Meunier *et al.,* 1988), or by reaction between Mg-rich carbonate and dioctahedral clay minerals (Hutcheon *et al.,* 1980; Hillier, 1993). In recent years it has been debated whether the transition from smectite to chlorite occurs as a continuous progressive transformation characterized by random and regular interlayering of different proportions of the end-member phases, as described by Bettison-Varga *et al.* (1991), or if such transition is more accurately described as discontinuous steps between discrete smectite, corrensite, and chlorite (Shau *et al.,* 1990; Hillier, 1993, 1995; Schiffman and Staudigel, 1995; Roberson *et al.,* 1999). Shau and Peacor (1992) suggested that the continuous transition occurs within incompletely recrystallized samples (*i.e.,* those affected by relatively low fluid/rock interactions), whereas for higher fluid/rock ratios the discontinuous transformation is favored, and only the discrete phases are present.

This paper describes the occurrence, mineral association, and crystal-chemical aspects of chlorite, corrensite, and micas in fluvio-lacustrine sediments from a stratigraphic profile through the Thitonian-Berriasian (Upper Jurassic-Lower Cretaceous) depositional sequence in the Cameros basin of northeast Spain. Dif-

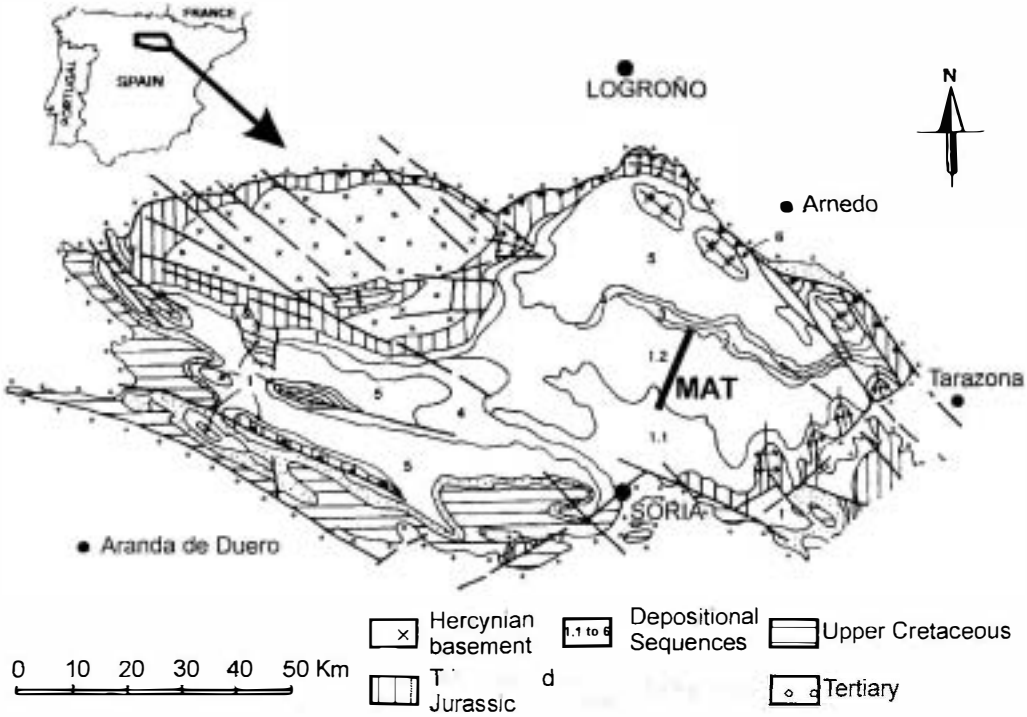

Figure 1. Geologic map of the study area, showing the location of the Matasejún profile (MAT). Modified after Guimerá *et al.* (1995).

ferences in the mineral assemblages and chemical composition of the phyllosilicates from diverse sedimentary facies are examined in detail to establish the possible mechanisms of formation of the phyllosilicates.

GEOLOGICAL SETTING AND SAMPLES

The Cameros basin represents the thickest sedimentary record within the Mesozoic basins of the Iberian Range for Late Jurassic to Early Cretaceous ages. Predominantly continental sediments of ≤9000 m accumulated in this extensional basin from the Tithonian to the Early Albian. Mas *et al.* (1993) considered these sediments as a megasequence bounded by major discontinuities divided into six depositional sequences (DS1 to DS6).

An outstanding feature of the Cameros basin is a low-grade metamorphic event, which according to K-Ar dating of authigenic illites (Casquet *et al.,* 1992) occurred during Middle to Late Cretaceous times (108–86 million years ago). On the basis of mineralogical, petrological, and fluid inclusions data, Casquet *et al.* (1992) related the metamorphism to the circulation of hot migratory fluids within the basin. The distribution of clay mineral assemblages and crystallinity data of illite and chlorite for the Latest Berriasian to Early Aptian depositional sequences (DS2 to DS5 following the schema of Mas *et al.,* 1993) indicate a progressive decrease in metamorphic grade from the depocentral sector to the borders of the basin (Barrenechea *et al.,* 1995; Alonso-Azcárate *et al.,* 1995). Both studies, together with the results of Alonso-Azcárate *et al.* (1999) on the formation mechanism of the sulfide deposits, are in good agreement with a hydrothermal origin of metamorphism.

During the Paleogene and Early Miocene, the Cameros basin was inverted by a north-directed neoformed thrust over the Tertiary sediments of the Ebro basin (≤30 km of displacement) and a system of thrusts at the southern margin over the Tertiary Duero basin (Mas *et al.,* 1993; Guimerá *et al.,* 1995).

The studied samples are mudstones, marls, and limestones collected from a thick stratigraphic cross-section (Matasejún profile, 1146 m) through most of the Tithonian-Berriasian depositional sequence (upper part of Tera Group and Oncala Group) in the depocentral area of the basin (Figure 1). According to Mas *et al.* (1993), this depositional sequence represents the beginning of the filling of the basin. A detailed description of the Matasejún profile is in Gómez Fernández (1993). This profile is characterized by an alternation of lacustrine marls and limestones with green, gray, and ocher mudstones and quartzites, which are flood-plain deposits from a meandering fluvial system. The lowest 250 m of the profile consist predominantly of limestones which contain ostracods and show evidence of frequent dessication. Scarce mudstones and

quartzites are interbedded with limestones. The overlying 600 m are dominated by gray, black, and green mudstones with variable proportions of interlayered channelized quartzites and less frequently with tabular gray and black limestones. A progressive increase in the proportion of marls and limestones is observed in the top of the profile, where gray laminated limestones are found rich in ostracods and bivalves.

METHODS

Bulk mineralogy was obtained from X-ray diffraction traces of non-oriented powder samples combined with petrographic observations. Approximately 100 g of each sample were ground in a tungsten-carbide swing-mill for 20 s. This short grinding time did not apparently affect the X-ray diffraction traces, which suggests the lack of structural damage of the phyllosilicates. Samples containing carbonate were treated with 5% acetic acid and washed with deionized water. The <2-μm size fraction was obtained using differential tubes and millipore filters. Following Ca-saturation and washing, air-dried oriented mineral aggregates were prepared by pipetting suspensions (~5 mg/cm^2) onto glass slides. Samples were solvated with ethylene glycol and, in some cases, were subjected to thermal treatment (550°C for 1 h).

Non-oriented powders and oriented clay aggregates (<2-μm size fraction) of each sample were examined in a Siemens D5000 diffractometer, equipped with a graphite monochromator, using the Siemens SOCABIM Diffract AT3.2 Software. The full-width at half-maximum peak height of illite and chlorite (IC and ChC, respectively) were determined to evaluate changes in diagenetic to low-grade metamorphic conditions. In some cases, the IC values were estimated by a deconvolution routine to overcome the overlap with illite-smectite mixed-layers. As suggested by Frey (1987), we will refer to the terms diagenesis, anchizone, and epizone on the basis of the IC values, according to the limits of Kubler (1967). Following calibration, the anchizone boundaries for the IC values are defined at indices of 0.42 and 0.25 °Δ2θ. These boundaries for the ChC values (0.21 and 0.28 °Δ2θ) are taken from a correlation by Alonso-Azcárate *et al.* (1995) of samples from the Iberian Chain.

Chemical compositions were determined using the JEOL JXA-8600 superprobe at the University of Basel. Si, Al, Ti, Fe, Mg, Mn, Ca, Na, and K were measured using wavelength-dispersive spectroscopy at an accelerating voltage of 15 kV, and a beam current of 10 nA. To minimize evaporation of light elements (*e.g.*, Na), the spot size was 6 μm. Data were corrected using the PROZA program. Back-scattered electron-microscope (BSEM) images were taken on the superprobe. The analyses of micas, corrensites, and chlorites were recalculated on the basis of 22, 25, and 28 oxygen atoms, respectively. Iron was considered as ferrous. Chlorite analyses were selected according to the chemical constraints of Zane *et al.* (1998) for metamorphic chlorites of greenschists-facies rocks: Na + K + Ca < 0.1 atoms per formula unit (apfu), total octahedral occupancy in the range 11.7–12.1 apfu, and Si ranging between 5.00–5.65 apfu.

RESULTS

The mineralogical components of the samples studied are given in Table 1. All samples in this profile contain quartz and white K-rich mica. Calcite is present in most samples from the bottom and top of the profile, but occurs in a very few samples elsewhere. Dolomite occurs in five samples from the top and one at the base and always with quartz and calcite. Most samples containing dolomite lack chlorite and/or corrensite. Small amounts of albite were also detected along the profile, except for samples MAT30, MAT34, and MAT35, which contain paragonite and Na-, K-rich mica. Reflected-light microscopy revealed relics of framboidal pyrite in some samples.

The clay minerals are dominated by illite, which occurs predominantly as the $2M_1$ polytype based on the method of Callière *et al.* (1982). However, some samples contained ≤25% of the $1M$ polytype. The mean d(060) value of the illite is 1.504 Å, with d(001) values ranging between 9.97–9.98 Å.

Chlorite is commonly present in the basal and middle parts of the profile. The chlorite is trioctahedral, with mean values for d(001) and d(060) of 14.18 and 1.536 Å, respectively. Corrensite is abundant and coexists with illite (Figure 2a) or with illite and chlorite (Figure 2b) in a relatively well-defined siliciclastic interval within the middle part of the stratigraphic profile (see Table 1). Corrensite never coexists with dolomite, but it does occur with calcite in a few samples. Corrensite displays a (001) reflection at 29 Å which shifts to 31 Å after ethylene-glycol solvation and rational higher-order reflections to the (0,0,10). The highly rational character of the basal reflections produces a mean coefficient of variability (CV) as proposed by Bailey (1982) of 0.60%. In three samples containing illite and chlorite, the (001) reflection of corrensite is not well defined in the air-dried preparation. However, the sharp peak near 31 Å after ethylene-glycol solvation is evidence for a regular interestratification of the chlorite and smectite components in these samples. The trioctahedral nature of at least one component is indicated by a strong d(060) reflection at 1.54 Å.

Paragonite and Na-, K-rich mica occur in three samples (lacking albite) from the top of the sequence. The low-order reflections of these phases overlap with the illite peaks, but the d(005) reflections at 1.96 and 1.92 Å (for Na-, K-rich mica and paragonite, respectively) are easily resolved from the illite 1.99-Å peak. On the basis of the IC and ChC data, these samples correspond to the limit between anchimetamorphic and epi-

Table 1. Variation in the mineralogical composition and lithology of the samples collected along the Matasejún stratigraphic cross-section. Quartz, calcite, dolomite, and albite contents were estimated from X-ray diffraction traces of unoriented mineral-aggregate samples, whereas the phyllosilicate contents were calculated from oriented aggregates of the <2-μm fraction. Presence of coalified organic matter was inferred from reflected-light microscopy and by flotation techniques. Major phase (****), frequent phase (***), minor phase (**), accessory phase (*).

Sample	Quartz	Calcite	Dolomite	Illite	Chlorite	Corrensite	Organic matter	Paragonite	Na-K-Mica	Albite	Lithology
MAT1	***	****		**	**						Marly limestone
MAT2	****	***		**	*					*	Finely laminated marl
MAT3	**	****		*	**					*	Gray marl
MAT4	****			**	*					*	Finely laminated mudrock
MAT6	****	**	***	**	*					*	Gray marl
MAT7	***	****		**	**					*	Ocher Marl
MAT8	****			***	**	*	*			*	Gray mudrock
MAT10	****			***	**					*	Mudrock
MAT11	****			**		**				*	Ocher mudrock
MAT13	****	*		**	***		*			*	Gray/black mudrock
MAT14	****	*		**	***		*			*	Gray/black mudrock
MAT15	****			**		***				*	Green mudrock
MAT16	****	*		**		****				*	Ocher mudrock
MAT17	****			**		***				*	Ocher mudrock
MAT18	*	****		*	*	**				**	Ocher mudrock
MAT19	****			**	**	*	*			*	Gray mudrock
MAT20	****			**	*	*	*			*	Gray mudrock
MAT21	****			**	*	**	*			*	Gray mudrock
MAT22	****			**	*	**	*			*	Gray mudrock
MAT23	****	*		**	**	*	*			*	Green mudrock
MAT25	****	**		**	**					*	Grey marly mudrock
MAT26	****	***		***	****		*			*	Gray sandy marl
MAT27	****	***		**	**					*	Gray marl
MAT28	****	**		**	***		*			*	Gray marl
MAT29	**	****	**	*	*					*	Limestone
MAT30	****			**				*	*		White sandy mudrock
MAT31	****	***	**	**						*	Limestone
MAT32	****	**	*	**						*	Gray marl
MAT33	*	****	*	**	*					*	Gray marl
MAT34	**	****		*				*	*		Limestone
MAT35	***	****	*	**						*	Limestone

metamorphic conditions, with mean values of 0.25 and 0.21 °Δ2θ (standard deviation of 0.02 for 35 samples), respectively.

Petrographic observation of polished thin sections using BSEM showed that most samples contain medium- to coarse-size (below the size of 35 × 10 μm) elongated grains of chlorite, mica, and chlorite-mica crystals, surrounded by fine-grained matrix or by irregular-shaped grains of quartz and albite (Figure 3). The angular shape of the larger phyllosilicate grains indicates that the chlorite-mica crystals result from the replacement of a detrital phyllosilicate precursor. However, no remnants of such precursors were recognized within the studied mudstones. Ti-oxide phases are commonly associated with the chlorite-mica crystals (Figure 3), and small zircon grains occur dispersed in the matrix. Corrensite is found as small crystals filling voids between quartz and albite grains, or within chlorite-mica crystals, where it occurs in association with Ti-oxide phases (Figure 3). Chlorite and mica form irregular intergrowths of varying thickness within the larger stacks, although the proportion of chlorite is slightly higher in most cases. The boundary between chlorite and mica domains within the crystals is usually difficult to establish. In samples from the lacustrine marls and limestones from the top of the stratigraphic profile where corrensite is lacking, the chlorite-mica crystals and chlorite grains are frequently in contact with calcite crystals.

Representative electron-microprobe analyses of chlorite, corrensite, and mica are presented in Table 2. Chlorites commonly show high octahedral occupancies, with totals near ideal for a trioctahedral mineral. The relative proportions of Fe^{2+} and Mg^{2+} show a strong inverse correlation (Figure 4), with the ferrous or magnesian content dependent on the position in the profile. Chlorite analyses from mudrocks from the middle of the stratigraphic profile show higher Fe^{2+} contents [with average Fe/(Fe + Mg) ratios of 0.56] than from the lacustrine carbonates from the base or top of the profile, where Fe/(Fe + Mg) ratios range between 0.18–0.37.

For a given sample, chlorite is richer in Fe^{2+} and poorer in Si than the corrensites (Figure 5). The Mg content is also higher in the chlorites, but the differences are much smaller. Consequently, the mean Fe/

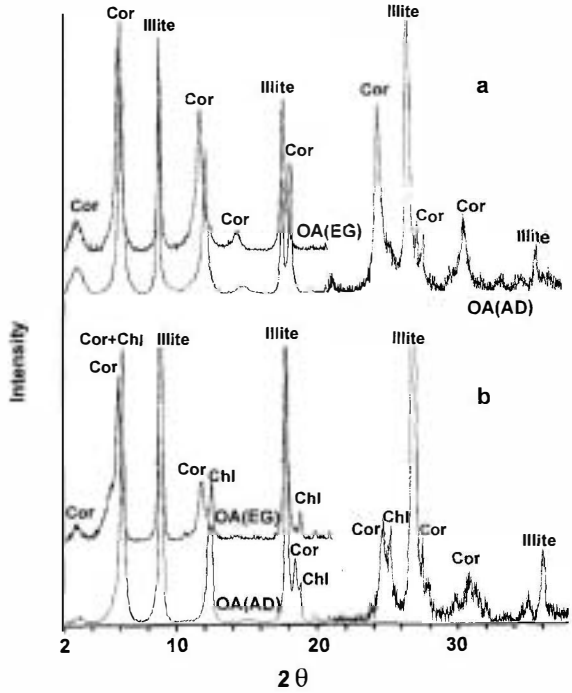

Figure 2. X-ray diffraction traces (after background subtraction) of air-dried (AD) and ethylene-glycol solvated (EG) oriented aggregates (<2 μm). (a) Sample MAT11, formed by corrensite (Cor) and illite, and (b) sample MAT21, with corrensite, illite, and chlorite (Chl).

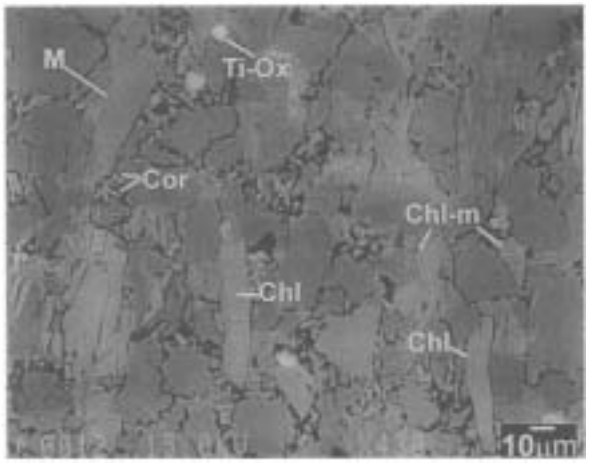

Figure 3. BSEM image of sample MAT22, with large (≤50 μm) chlorite (Chl), mica (M), and chlorite-mica stack (Chl-m) crystals. Corrensite (Cor) is found as small grains (<10 μm) among feldspar and quartz. Ti oxides (Ti-Ox) are frequently associated with the chlorite-mica crystals.

(Fe + Mg) ratios are slightly lower in the corrensites than in the chlorites, averaging 0.51 and 0.56, respectively (Table 2). Corrensite has higher Si and Na + K + Ca contents than chlorite and lower octahedral totals (Figure 6), whereas the Al(total) is similar in both phases (Figure 5). When calculated on the basis of 25 oxygen atoms, the sums of non-interlayer cations are close to 17. Note the high K contents for the corrensite

Table 2. Representative electron-microprobe analyses of chlorite (Chl), corrensite (Cor), and mica. Samples MAT11 and MAT22 correspond to mudrocks from siliciclastic sediments, whereas samples MAT8 and MAT28 were collected in the lacustrine carbonates from the base and top of the profile, respectively.

	MAT11 Chl	MAT22 Chl	MAT28 Chl	MAT8 Chl	MAT11 Cor	MAT22 Cor	MAT11 Mica	MAT22 Mica	MAT28 Mica	MAT8 Mica
SiO_2	23.55	25.7	27.26	27.17	31.41	30.82	43.34	46.87	49.34	47.83
TiO_2	0.06	0.05	0.09	0.03	0.66	0.08	0.31	0.21	0.21	0.28
Al_2O_3	22.34	21.36	21.30	21.02	21.67	20.56	34.16	37.05	32.63	29.71
FeO	29.26	28.88	19.91	12.76	21.81	24.12	1.74	1.37	1.23	1.52
MnO	0.25	0.15	0	0.03	0.14	0.14	0	0	0.06	0.01
MgO	11.46	13.07	19.42	24.20	10.63	12.13	0.97	0.72	2.51	2.64
CaO	0.01	0.06	0.14	0	0.59	0.40	0	0	0.12	0
Na_2O	0.04	0	0	0	0.10	0.15	0.54	0.71	0.34	0.26
K_2O	0.02	0.07	0.02	0.04	1.26	0.81	9.02	9.6	9.66	8.42
Total	86.99	89.34	88.14	85.25	88.27	89.21	90.08	96.53	96.10	90.67
Si	5.13	5.41	5.53	5.50	5.70	5.60	6.08	6.12	6.46	6.60
^{IV}Al	2.87	2.59	2.47	2.50	2.30	2.40	1.92	1.88	1.54	1.40
Ti	0.01	0.01	0.01	0.00	0.09	0.01	0.03	0.02	0.02	0.03
^{VI}Al	2.87	2.70	2.62	2.51	2.33	2.00	3.74	3.81	3.49	3.43
Fe	5.33	5.08	3.38	2.16	3.31	3.67	0.20	0.15	0.13	0.18
Mn	0.05	0.03	0.00	0.01	0.02	0.02	0.00	0.00	0.01	0.00
Mg	3.72	4.10	5.87	7.30	2.87	3.29	0.20	0.14	0.49	0.54
Ca	0.00	0.01	0.03	0.00	0.11	0.08	0.00	0.00	0.02	0.00
Na	0.02	0.00	0.00	0.00	0.04	0.05	0.15	0.18	0.09	0.07
K	0.01	0.02	0.01	0.01	0.29	0.19	1.62	1.60	1.61	1.48
Fe/(Fe + Mg)	0.59	0.55	0.37	0.23	0.54	0.53	0.50	0.52	0.22	0.24
$^{IV}Al/^{VI}Al$	1.00	0.96	0.94	0.99	0.99	1.20	0.51	0.49	0.44	0.41
^{VI}Al + Fe + Mg + Mn	11.97	11.91	11.87	11.98	8.53	8.98	4.14	4.10	4.12	4.15
(K + Na + Ca)	0.02	0.03	0.04	0.01	0.44	0.32	1.76	1.78	1.72	1.55

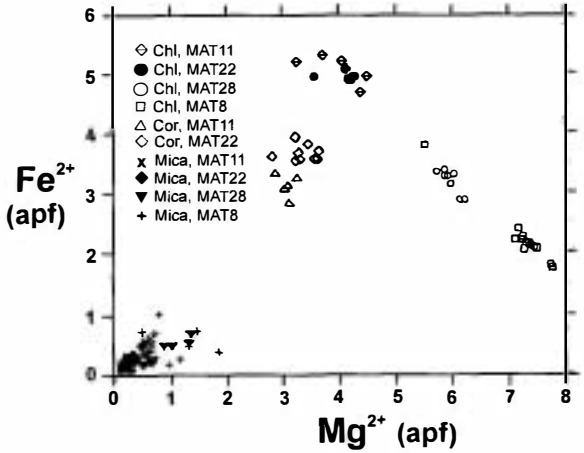

Figure 4. Plot of Mg *vs.* Fe^{2+} (atoms per formula unit) for chlorite, corrensite, and mica crystals analyzed in different samples. Note the clear trend between Mg and Fe in chlorites. Samples MATl 1 and MAT22 correspond to mudrocks from siliciclastic sediments, whereas samples MAT8 and MAT28 are from the lacustrine carbonates from the base and the top of the profile, respectively.

analyses. Examples of corrensites where K is a major component were reported by Brigatti and Poppi (1984), Shau and Peacor (1992), and Jiang and Peacor (1994a).

Muscovite within the chlorite-mica crystals has significant Ti and relatively low Na and Ca contents. The Fe/(Fe + Mg) ratios follow roughly a similar distribution to that described above for the chlorites, with mean values of 0.5 in the mudrocks from the middle of the profile and 0.34 in the lacustrine marls and limestones from the base and top of the sequence (Table 2).

DISCUSSION

There is a clear control of the sedimentary facies on the phyllosilicate assemblages. Samples containing corrensite (+ illite ± chlorite) are restricted to a well-defined siliciclastic interval in the middle part of the profile. This interval is dominated by mudstones with variable amounts of quartzites and less frequently with tabular gray and black limestones. No corrensite and minor amounts of chlorite occur in the lacustrine carbonates from the base and the top of the profile where calcite and dolomite are widespread. The importance of sedimentary facies for the distribution of clay-mineral assemblages (and consequently for the estimation of metamorphic conditions) was noted by Barrenechea *et al.* (1995) and Alonso-Azcárate *et al.* (1995) for the metasediments of the overlying Late-Berriasian to Early-Aptian depositional sequences in the Cameros basin.

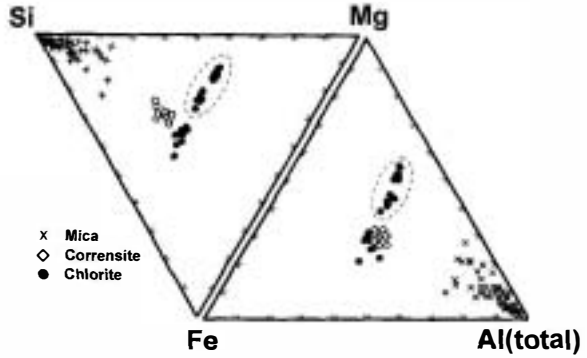

Figure 5. Plot of the compositions of chlorite, corrensite, and mica crystals analyzed in different samples on the Si-Fe^{2+}-Mg and Al(total)-Fe^{2+}-Mg ternary diagrams. The dashed line encloses Mg-rich chlorite compositions from samples without corrensite.

Origin of chlorite and corrensite

In the lacustrine marls and limestones from the base and top of the profile, the inverse relationship observed for the amounts of chlorite and dolomite (Table 2) is noteworthy. In addition, chlorite has a high Mg content. These data indicate that chlorite and chlorite-mica crystallization involves the destabilization of dolomite, because dolomite provides a Mg^{2+}-rich source with little Fe^{2+}. Hillier (1993) observed a similar relation for lacustrine mudrocks from the Orcadian basin, and he suggested that chlorites and corrensites formed in his samples from a reaction between dolomite (to provide Fe and Mg) and detrital dioctahedral clay minerals and quartz (to provide Si and Al). This reaction, also proposed by Hutcheon *et al.* (1980), implies the formation of calcite from lacustrine facies:

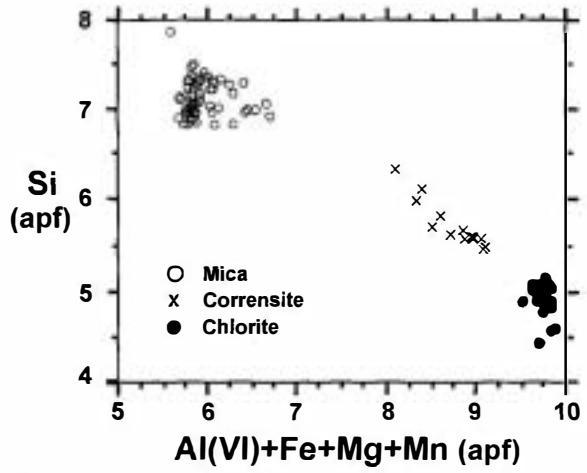

Figure 6. Plot of Si *vs.* the sum of octahedral cations (calculated on the basis of 25 oxygen atoms) for chlorite, corrensite, and mica crystals analyzed in different samples.

$$15\text{Dolomite} + 2\text{Illite} + 3\text{Quartz} + 11\text{Water} = 3\text{Chlorite} + 15\text{Calcite} + 2K^+ + 2OH^- + 15CO_2. \quad (1)$$

A similar reaction may be applied here because calcite-bearing samples contain chlorite and both phases are frequently in contact. Thus, reactions involve a breakdown of dolomite and further reaction with illite or illite-smectite mixed-layered phases, followed by direct precipitation in the matrix and replacement of detrital phyllosilicate grains, to yield Mg-rich chlorites and calcite.

However, the absence of dolomite and calcite and the Fe-rich chlorites and corrensites observed in the mudrocks of the middle part of the profile are difficult to explain by Reaction (1). Chlorite, corrensite, and micas form parallel to sub-parallel intergrowths which are commonly associated with Ti oxides. Chlorite and corrensite occur also as small crystals filling voids between albite and quartz grains. In addition, the compositions of chlorite, corrensite, and mica within a given sample follow a similar trend, especially with respect to Fe/Mg ratios. These features suggest a formation mechanism of the phyllosilicates by replacement of a detrital phyllosilicate precursor, most probably igneous biotite. A similar occurrence of corrensite, chlorite, and chlorite-mica crystals by replacement of detrital biotite in a prograde sequence of pelitic rocks from the Gaspé Peninsula in Quebec was described by Jiang and Peacor (1994a, 1994b). They suggested two possible mechanisms of formation for chlorite and corrensite during diagenetic alteration: 1) layer-by-layer replacement of biotite, and 2) dissolution-transport-precipitation. Subsequent prograde evolution of illite and corrensite-chlorite produces muscovite and chlorite, respectively. They also found that biotite alteration is closely related to the formation of titanite and magnetite in diagenetic rocks, and pyrite, calcite, and Ti oxides in the higher-grade rocks. Similarly, Li *et al.* (1998) described the formation of sulfides during alteration of biotite in a Middle Triassic ash bed from South Otago, New Zealand. Textural relationships, together with compositional data (presence of Ti oxides, Fe/Mg ratios of the phyllosilicates, *etc.*), suggest a similar formation mechanism for chlorite, corrensite, and mica from the Cameros basin. Although no remnants of detrital biotite were identified, unaltered detrital biotite grains in the Western Sector of the Cameros basin were found by Santos and Blanco (1993). Furthermore, Mata *et al.* (1999) suggested that igneous biotite is probably the precursor for phyllosilicate intergrowths of the overlying metasediments of the Late Berriasian to Early Aptian depositional sequences.

Some aspects of the origin and distribution of corrensite remain unclear, such as the factors controlling the presence of coexisting phases. The most significant difference between samples containing corrensite + chlorite and those where corrensite occurs as the only trioctahedral phyllosilicate is the presence of organic matter in the former and not in the latter (Table 1). These differences suggest local changes in oxygen fugacity, $f(O_2)$, conditions. Well-preserved organic matter is indicative of reducing conditions. In an experimental study on the stability of various dioctahedral and trioctahedral phyllosilicates, Velde (1977) noted the importance of the Al^{3+} and/or Fe^{3+} content of the mineral assemblage (estimated indirectly from the presence or absence of organic matter). He concluded that corrensite crystallization is related to the Fe^{3+} content. Surdam and Crossey (1985) suggested that $f(O_2)$ and $f(CO_2)$ conditions during diagenesis are controlled by an oxidation-reduction reaction involving clay transformations and kerogen maturation. The formation of corrensite instead of chlorite in hydrothermal veins within a Paleozoic granite from the Vosgues Massif is also related to redox conditions, as indicated by the presence of hematite (Meunier *et al.,* 1988). Finally, Jiang and Peacor (1994a) suggested that chlorite or corrensite in pelitic rocks depends on local changes of $f(O_2)$ and $f(CO_2)$, possibly related to decarboxilation reactions of the organic matter. Thus, we suggest that oxidizing conditions favored corrensite alone in our samples, whereas the occurrence of corrensite + chlorite was related to reducing conditions.

Compositional variations of chlorite and corrensite

Both Mg and Fe-rich chlorites were found in samples from the profile, with variations in composition dependant upon the sedimentary facies. However, chlorite compositions within a given sample are nearly homogeneous. Hillier (1993) suggested that coexisting Mg and Fe-rich chlorites within a diagenetic mudrock are indicative of disequilibrium at the microscopic scale. In contrast, Jiang and Peacor (1994b) and Jiang *et al.* (1994) described heterogeneous chlorite compositions in diagenetic and anchizonal samples, which become progressively more homogeneous in the epizone. In our study, metamorphic conditions estimated from IC and ChC data are between anchizone and epizone, which is consistent with the observed homogeneity in chlorite compositions within a given sample. Differences in Fe/(Fe + Mg) ratios seem to be related to the composition of the precursor material (*e.g.,* presence of dolomite, *etc.*), which is intimately linked to the sedimentary facies. As shown by Zane *et al.* (1998), the bulk-rock chemistry controls the composition of metamorphic chlorites, and it largely obscures systematic compositional changes caused by temperature and pressure.

As mentioned above, corrensite is commonly associated with Fe-rich chlorite. The analyses of corrensite are similar to those of Inoue (1985), Shau *et al.* (1990),

Shau and Peacor (1992), Jiang and Peacor (1994b), and Schiffman and Staudigel (1995), with higher Si and Na + K + Ca contents and slightly lower values of Fe/(Fe + Mg) than chlorites. Higher substitutions of octahedral Fe^{2+} for Mg^{2+} in the chlorites may compensate for the distortions introduced by the substitution of the larger Al^{3+} cation for Si^{4+} in the tetrahedral sheet (Shau *et al.,* 1990). However, Hillier (1993), Bettison-Varga *et al.* (1991), and Bettison-Varga and Mackinnon (1997) found no changes in the Fe/Mg ratio of coexisting chlorites and corrensites. Our results indicate a clear difference between chlorite and corrensite compositions, with well-defined ranges for each phase (Figures 4 and 5).

Implications on the type and conditions of the metamorphism

Casquet *et al.* (1992), Barrenechea *et al.* (1995), and Alonso-Azcárate *et al.* (1995) suggested the importance of the circulation of hot migratory fluids in the development of metamorphism in the Cameros basin based on the following observations: (1) the age of the main thermal event (Middle to Late Cretaceous), which clearly post-dates the filling of the basin, (2) the close relationship between physical characteristics of the sedimentary facies (*i.e.,* permeability, porosity) and the distribution of mineral assemblages (and IC, ChC), (3) the abnormally high geothermal gradient, and (4) the presence of large concentrations of large pyrite crystals with inclusions of chloritoid (Alonso-Azcárate *et al.,* 1999) in the Barremian depositional sequence at the southeast sector of the basin.

Corrensite is commonly stable at deep-diagenetic or low-anchimetamorphic conditions. However, the IC and ChC values in these samples from the Matasejún profile are characteristic for the boundary between anchimetamorphism and epimetamorphism. In addition, low-grade metamorphic conditions were inferred by Barrenechea *et al.* (1995) for the chloritoid-bearing mudstones of the overlying Late Berriasian-Valanginian depositional sequence in the same area. Thus, the corrensite in our samples appears to have formed out of its stability field. In contrast, Hillier (1993) showed that no direct relationship exists between the transformation of corrensite to chlorite and pressure and temperature during diagenesis and prograde metamorphism. Corrensite in clastic sedimentary rocks occurs in a range of temperatures much lower than in hydrothermally altered rocks (Frey, 1987).

On the basis of the above discussion, we suggest that the formation of corrensite was related to a temperature rise occurring over a relatively short period. The different reaction rates for the phases present explain the apparent discrepancy between the metastable mineral assemblage and the IC and ChC data, suggesting formation between the anchizone and epizone. If these rocks belong to a typical prograde sequence of diagenesis to low-grade metamorphism, corrensite would not exist and chlorite would be present. Presumably, hot migratory fluids can provide a sufficient source of heat over a short period. Thus, the presence of corrensite is probably additional evidence for the hydrothermal character of the metamorphism in the Cameros basin.

Note the absence of random chlorite-smectite interlayering within these mudrocks. Shau and Peacor (1992) suggested that a continuous transition (characterized by random and regular interlayering of different proportions of smectite and chlorite) occurs in samples affected by relatively low fluid/rock interaction, whereas for higher fluid/rock ratios a discontinuous transformation is favored, and only discrete phases (chlorite ± corrensite ± smectite) are present. This suggestion usually involves materials from hydrothermal alteration of basaltic rocks where there is evidence of pervasive fluid interaction. However, rocks from the Cameros basin presumably have low fluid/rock ratios, because corrensite occurs within compacted mudstones interbedded with sandstones, and thus these rocks are least likely to have interacted with large volumes of water. Hence, the hydrothermal event would have largely been a thermal event in the mudstones.

Nevertheless, the permeability in these mudrocks may have been enhanced by a combination of the heterolithic character of these sediments (mudstone/sandstone; marls/limestone), as a consequence of frequent lateral-facies changes, and by widespread hydroplastic microfractures produced at an early stage and preserved during compaction of the sediments. These microfractures were first described by Guiraud (1983) in different parts of the Cameros basin. In a study of the large pyrite deposits from the eastern sector of the basin, Alonso-Azcárate *et al.* (1999) suggested that these fractures were responsible for an increase in the permeability of the mudrocks, and related their distribution to geometry and size of the deposit. Assuming that the permeability of the mudrocks was enhanced by the above mechanisms, it is possible to relate the absence of random chlorite-smectite interlayering to a high fluid/rock ratio.

ACKNOWLEDGMENTS

This study was supported by the Spanish DGICYT through project PB97-0298, and by the Universidad Complutense de Madrid through a grant to J.F. Barrenechea. Critical reviews by R. Lahann, H. Roberson, and D.M. Moore helped greatly to improve the manuscript.

REFERENCES

Almon, W.R., Fullerton, L.B., and Davies, D.K. (1976) Pore space reduction in Cretaceous sandstones through chemical precipitation of clay minerals. *Journal of Sedimentary Petrology,* **46,** 89–96.

Alonso-Azcárate, J., Barrenechea, J.F., Rodas, M., and Mas, J.R. (1995) Comparative study of the transition between very low grade and low grade metamorphism in siliciclastic

and carbonate sediments. Early Cretaceous, Cameros Basin (North Spain). *Clay Minerals,* **30,** 407–419.

Alonso-Azcárate, J., Rodas, M., Bottrell, S.H., Raiswell, R., Velasco, F., and Mas, J.R. (1999) Pathways and distances of fluid flow during low-grade metamorphism: Evidence from pyrite deposits of the Cameros Basin, Spain. *Journal of Metamorphic Geology,* **17,** 339–348.

April, R.H. (1981) Trioctahedral smectite and interstratified chlorite/smectite in Jurassic strata of the Conneticut Valley. *Clays and Clay Minerals,* **29,** 31–39.

Bailey, S.W. (1982) Nomenclature for regular interstratifications. *American Mineralogist,* **67,** 394–398.

Barrenechea, J.F., Rodas, M., and Mas, J.R. (1995) Clay mineral variation associated with diagenesis and low grade metamorphism of Early Creataceous sediments in the Cameros Basin, Spain. *Clay Minerals,* **30,** 119–133.

Bettison-Varga, L. and Mackinnon, I.D.R. (1997) The role of randomly mixed-layered chlorite/smectite in the transformation of smectite to chlorite. *Clays and Clay Minerals.* **45,** 506–516.

Bettison-Varga, L., Mackinnon, I.D.R., and Schiffman, P. (1991) Integrated TEM, XRD and microprobe investigation of mixed-layered chlorite/smectite from the Point Sal Ophiolite, California. *Journal of Metamorphic Geology,* **9,** 711–721.

Bodine, M.W. and Madsen, B.M. (1987) Mixed-layer chlorite/smectites from a Pennsylvanian evaporite cycle, Grand County, Utah. In *Proceedings of the International Clay Conference Denver, 1985,* L.G. Schultz, H. van Olphen, and F.A. Mumpton, eds., The Clay Minerals Society, Denver, Colorado, 85–93.

Brigatti, M.F. and Poppi, L. (1984) Crystal chemistry of corrensite: A review. *Clays and Clay Minerals,* **32,** 391–399.

Caillère, S., Henin, S., and Rautereau, M. (1982) *Minèralogie des Argiles. I. Structure et Priopiétés Physica Chimiques.* Masson ed., Paris, 184 pp.

Casquet, C., Galindo, C., González Casado, J.M., Alonso, A., Mas, J.R., Rodas, M., García, E., and Barrenechea, J.F. (1992) El metamorfismo en la Cuenca de los Cameros. Geocronología e implicaciones tectónicas. *Geogaceta,* **11,** 22–25.

Chang, H.K., Mackenzie, F.T., and Schoonmaker, J. (1986) Comparisons between the diagenesis of dioctahedral and trioctahedral smectite, Brazilian offshore basins. *Clays and Clay Minerals,* **34,** 407–423.

Frey, M. (1987) Very low-grade metamorphism of clastic sedimentary rocks. In *Low-Temperature Metamorphism,* M. Frey, ed., Blackie and Sons, Glasgow, 9–58.

Gómez Fernández, J.C. (1993) Análisis de la Cuenca sedimentaria de los Cameros durante sus etapas iniciales de relleno en relación con su evolución paleogeográfica. Ph.D. thesis, Universidad Complutense de Madrid, 343 pp.

Guimerá, J., Alonso, A., and Mas, J.R. (1995) Inversion of an extensional-ramp basin by a neoformed thrust: The Cameros basin (N Spain). In *Basin Inversion,* J.G. Buchanan and P.G. Buchanan, eds., Geological Society Special Publication 88, London, 433–453.

Guiraud, M. (1983) Evolution tectono-sédimentaire du basin Wealdien (Crétacé inférieur) en relais de décrochements de Logroño-Soria (NW Espagne). Ph.D. thesis, Université des Sciences et Techniques de Languedoc, Montpellier, 183 pp.

Hillier, S. (1993) Origin, diagenesis, and mineralogy of chlorite minerals in Devonian lacustrine mudrocks, Orcadian Basin, Scotland. *Clays and Clay Minerals,* **41,** 240–259.

Hillier, S. (1995) Mafic phyllosilicates in low-grade metabasites. Characterization using deconvolution analysis—Discussion. *Clay Minerals.* **30,** 67–73.

Hutcheon, I., Oldershaw, A., and Ghent, E.D. (1980) Diagenesis of Cretaceous sandstones of the Kootenay Formation at Elk Valley (Southeast British Columbia) and Mt. Allan (Southwest Alberta). *Geochimica et Cosmochimica Acta,* **44,** 1425–1435.

Inoue, A. (1985) Chemistry of corrensite: A trend in composition of trioctahedral chlorite/smectite during diagenesis. *Journal of the College of Arts and Sciences, Chiba University,* **B-18,** 69–82.

Jiang, W.T. and Peacor, D.R. (1994a) Formation of corrensite, chlorite and chlorite-mica stacks by replacement of detrital biotite in low-grade pelitic rocks. *Journal of Metamorphic Geology,* **12,** 867–884.

Jiang, W.T. and Peacor, D.R. (1994b) Prograde transitions of corrensite and chlorite in low-grade pelitic rocks from the Gaspé Peninsula, Quebec. *Clays and Clay Minerals,* **42,** 497–517.

Jiang, W.T., Peacor, D.R., and Buseck, P.R. (1994) Chlorite geothermometry?—Contamination and apparent octahedral vacancies. *Clays and Clay Minerals,* **42,** 593–605.

Kubler, B. (1967) La cristallinité de l'illite et les zones tout á fait supérieures du métamorphisme. *Etages Techtoniques, Coll Neuchâtel,* 105–122.

Li, G., Peacor, D.R., and Essene, E.J. (1998) The formation of sulfides during alteration of biotite to chlorite-corrensite. *Clays and Clay Minerals,* **46,** 649–657.

Mas, J.R., Alonso, A., and Guimerá, J. (1993) Evolución tectonosedimentaria de una cuenca extensional intraplaca: La cuenca finijurásica-eocretácica de Los Cameros (La Rioja-Soria). *Revista de la Sociedad Geológica de España,* **6,** 129–144.

Mata, M.P., López-Aguayo, F., Gil-Imaz, A., and Pocoví, A. (1999) Intercrecimientos de filosilicatos en la Cuenca de Cameros y su relación con la génesis de la esquistosidad en la etapa metamórfica de bajo grado. *Geogaceta,* **24,** 227–230.

Meunier, A., Clement, J.I., Bouchet, A., and Beaufort, D. (1988) Chlorite-calcite and corrensite-dolomite crystallization during two superimposed events of hydrothermal alteration in the "Les Crêtes" granite, Vosgues, France. *Canadian Mineralogist,* **26,** 413–426.

Roberson, H.E., Reynolds, R.C., Jr., and Jenkins, D.M. (1999) Hydrothermal synthesis of corrensite: A study of the transformation of saponite to corrensite. *Clays and Clay Minerals,* **47,** 212–218.

Santos, G. and Blanco, J.A. (1993) Paleosuelos y paleoalteraciones del Weald de la zona oeste de la Cuenca de Cameros (borde SW de la Sierra de la Demanda). *Cuadernos de Geologia Ibérica,* **17,** 185–206.

Schiffman, P. and Staudigel, H. (1995) The smectite to chlorite transition in a fossil seamount hydrothermal system: The basement complex of La Palma, Canary Islands. *Journal of Metamorphic Geology,* **13,** 487–498.

Schmidt, S.Th. and Robinson, D. (1997) Metamorphic grade and porosity and permeability controls on mafic phyllosilicate distributions in a regional zeolite to greenschist facies transition of the North Shore Volcanic Group, Minnesota. *Geological Society of America Bulletin,* **109,** 683–697.

Shau, Y.H. and Peacor, D.R. (1992) Phyllosilicates in hydrothermally altered basalts from DSDP Hole 504B, Leg 83—a TEM and AEM study. *Contributions to Mineralogy and Petrology,* **112,** 119–133.

Shau, Y.H., Peacor, D.R., and Essene, E.J. (1990) Corrensite and mixed-layer chlorite/corrensite in metabasalt from northern Taiwan: TEM/AEM, EMPA, XRD, and optical studies. *Contributions to Mineralogy and Petrology,* **105,** 123–142.

Surdam, R.C. and Crossey, L.J. (1985) Mechanisms of organic/inorganic interactions in sandstones/shale sequences. In *Relations of Organic Matter and Mineral Diagenesis,* D.L. Gautier, Y.K. Kharaka, and R.C. Surdam, eds., Society

of Economic Paleontologists and Mineralogists, Tulsa, Oklahoma, 177–232.

Velde, B. (1977) A proposed phase diagram for illite, expanding chlorite, corrensite and illite-montmorillonite mixed layered minerals. *Clays and Clay Minerals,* **25,** 264–270.

Zane, A., Sassi, R., and Guidotti, C.V. (1998) New data on metamorphic chlorite as a petrogenetic indicator mineral, with special regard to greenschists-facies rocks. *Canadian Mineralogist,* **36,** 713–726.

E-mail of corresponding author: barrene@eucmax.sim.ucm.es